Journal of Power Sources 364 (2017) 121–129

Contents lists available at ScienceDirect

Journal of Power Sources

journal homepage: www.elsevier.com/locate/jpowsour

Unraveling the effect of exposed facets on voltage decay and capacity fading of Li-rich layered oxides

Dong Luo [a], Pei shi [a], Shaohua Fang [a, c, *], Li Yang [a, b, c, **], Shin-ichi Hirano [b]

[a] School of Chemistry and Chemical Engineering, Shanghai Jiao Tong University, Shanghai 200240, China
[b] Hirano Institute for Materials Innovation, Shanghai Jiao Tong University, Shanghai 200240, China
[c] Shanghai Electrochemical Energy Devices Research Center, Shanghai 200240, China

HIGHLIGHTS

- Two nanoplates with exposed (101) or (001) facets are prepared.
- Effect of exposed facets on voltage decay and capacity fading of LLOs is unraveled.
- Large area of active surface will accelerate electrochemical corrosion of LLOs.
- Phase transformation of LLOs can be mitigated by increasing the area of inactive surface.
- We discover Co and Ni are easier to react with electrolyte than Mn.

GRAPHICAL ABSTRACT

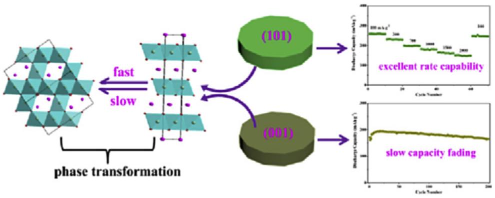

ARTICLE INFO

Article history:
Received 26 May 2017
Received in revised form
10 July 2017
Accepted 22 July 2017

Keywords:
Exposed facets
Li-rich layered oxides
Phase transformation
Electrochemical corrosion
Voltage decay and capacity fading

ABSTRACT

In this work, the effect of exposed facets on voltage decay and capacity fading of Li-rich layered oxides (LLOs) is unraveled via two nanoplates which are prepared by very similar co-precipitated-precursor method. The top-bottom surface of one nanoplate is (101) facet (S101 sample, active plane) and the other is exposed (001) facet (S001 sample, inactive plane). Although S101 sample delivers an excellent rate capability (149 mA h g^{-1} at 2000 mA g^{-1}), both its voltage and capacity decrease faster than S001 sample. TEM, HRTEM, XPS and XRD of cycled samples demonstrate: (1) Large area of active surface will accelerate electrochemical corrosion and phase transformation of LLOs and (2) electrochemical corrosion and phase transformation of LLOs with large area of inactive surface can be mitigated, leading to slow voltage decay and capacity fading. In addition, we discover Co and Ni are easier to react with electrolyte than Mn. Therefore, suitable facets and compositions may be more useful for improving the electrochemical performance of LLOs.

© 2017 Published by Elsevier B.V.

1. Introduction

The mass application of Li-ion batteries in the electric vehicle and large-scale energy storage is greatly limited by the availability of high-energy density cathodes. Therefore, the development of cathodes with high performance is urgently needed [1]. In this regard, Li-rich layered oxides (LLOs, $xLi_2MnO_3 \cdot (1-x)LiMO_2$ or $Li_{1+x}M_{1-x}O_2$, M = Mn, Co, Ni) have been widely investigated due to

---

* Corresponding author. School of Chemistry and Chemical Engineering, Shanghai Jiao Tong University, Shanghai 200240, China.
** Corresponding author. School of Chemistry and Chemical Engineering, Shanghai Jiao Tong University, Shanghai 200240, China.
E-mail addresses: housefang@sjtu.edu.cn (S. Fang), liyangce@sjtu.edu.cn (L. Yang).

http://dx.doi.org/10.1016/j.jpowsour.2017.07.078
0378-7753/© 2017 Published by Elsevier B.V.

their high specific capacity (ca. 250 mA h g^{-1}) and low cost [2,3]. The high specific capacity of LLOs originates from the electrochemical activation of Li_2MnO_3 component over 4.5 V [4,5]. However, the activation of Li_2MnO_3 component leads to high irreversible capacity loss and surface rearrangement of LLOs [6]. In LLO cathodes, Li-ions can only transport along the plane groups paralleled to the (001) facet [7]. It makes many characters of LLOs, such as rate capability and element segregations, have a close relation with exposed facets.

Up to now, literature have demonstrated that high percentage of active exposed planes, which have unimpeded pathways for Li-ions transportation, can help to optimize the rate capability of LLOs [8,9]. For instance, Wu et al. and Sun's group have shown that the rate capability of LLO nanoplates can be greatly improved by increasing the percentage of {010} active exposed planes [10,11]. In addition, Wang's group and Nanda et al. have found that both element segregations and phase transformation of LLOs are facet-dependent [12–14]. For element segregations and phase transformation, they are the most undesirable phenomena since they will result in voltage decay and capacity fading of LLOs [15–17]. However, the effect of inactive and active facets on element segregations and phase transformation of LLOs is far from clear. This is because LLOs with exposed inactive or active planes used to do the above study should be prepared by very similar method to ensure a single variable. It greatly enhances the difficulty of the study on the role of inactive and active facets in element segregations and phase transformation of LLOs.

In this work, two nanoplates are prepared by very similar co-precipitated-precursor method. The top-bottom surface of one nanoplate is (101) facet (S101 sample, active plane) and the other is exposed (001) facet (S001 sample, inactive plane). Electrochemical test suggests the rate capability of S101 sample is better than that of S001 sample. It is due to the active exposed plane which can shorten the transport distance of Li-ions in electrode materials. However, both the capacity and voltage of S101 sample decrease much faster than those of S001 sample. This is because large area of inactive surface can mitigate electrochemical corrosion and phase transformation of LLOs in terms of the discussion of TEM, HRTEM, XPS and XRD for cycled samples. In addition, we discover Co and Ni are easier to react with electrolyte than Mn.

2. Experimental section

2.1. Sample synthesis

Two LLO nanoplates were prepared by very similar co-precipitated-precursor method. Analytical grade chemicals of nickel sulfate ($NiSO_4 \cdot 6H_2O$), manganese sulfate ($MnSO_4 \cdot H_2O$), cobalt sulfate ($CoSO_4 \cdot 7H_2O$), sodium hydroxide (NaOH), diglycol (NMP: *N*-methyl pyrrolidinone), and ammonium hydroxide (NH_4OH) were chosen as the starting materials. For synthesis of the nanoplate with exposed (101) plane, 1825.4 mg $MnSO_4 \cdot H_2O$, 1209.1 mg $NiSO_4 \cdot 6H_2O$, 1293.1 mg $CoSO_4 \cdot 7H_2O$, and 50 mL NMP were dissolved in 100 mL deionized water to form aqueous solution. The mixed solution of 20 mL NaOH (2 mol L^{-1}) and 5 mL ammonia was added slowly in the above solution under stirring. After stirring for 5 min, 20 mL de-ionized water and 5 mL NaOH (2 mol L^{-1}) mixed solution were added slowly again. Then, 15 mL ammonia was dropped into after stirring for 20 h. The whole precipitation process was performed under N_2 gas. Finally, the obtained hydroxide precipitates were filtrated, washed with distilled water, and then dried at 160 °C for 12 h. These precipitates were respectively mixed with 1123.7 mg $LiOH \cdot H_2O$, calcined at 900 °C for 12 h, and then quenched to room temperature. This sample was named as S101. The synthesis of the nanoplate with exposed (001) plane was almost the same with that of the sample S101, except that 50 mL NMP was replaced by 50 mL diglycol. We named this sample as S001.

2.2. Sample characterization

Crystalline phases of the as-prepared samples were identified by X-ray diffraction measurement (XRD, Rigaku, D/max-Rbusing Cu K radiation) laser Raman spectroscopy (Renishaw in Via). The morphology and size of the samples were determined by field emission scanning electron microscopy (SEM) on a JEOL JSM-7401F instrument under an acceleration voltage of 5 kV and transmission electron microscopy (TEM) on a JEOL JEM-2010 apparatus with an acceleration voltage of 200 kV. The valence state of elements was further investigated by X-ray photoelectron spectroscopy (XPS) experiments measured on an AXIS ULTRA DLD instrument, using aluminum K X-ray radiation. Raman spectra were acquired by dispersive Raman Microscope (Senterra R200-L, Bruker Optics) using a solid-state 532 nm excitation laser.

2.3. Electrochemical test

Electrochemical performance of the samples was evaluated using the CR-2016-type coin cell. The cathode materials were prepared as follows: as-prepared sample powders, carbon black, and polyvinylidene fluoride (PVDF) were mixed in a weight ratio of 8:1:1. The resulting slurry was coated on Al foil and vacuum dried at 110 °C for 12 h. In an argon-filled glove box (H_2O and $O_2 < 1$ ppm), the cells were assembled using lithium foil as the anode, a polymer separator and 1 M $LiPF_6$ in EC:DMC (1:1 in volume) as the electrolyte. The cell was charged and discharged galvanostatically on a CT2001a cell test instrument (LAND Electronic Co.) in a voltage range of 2.0–4.8 V at room temperature.

3. Results and discussion

3.1. Structure and morphology of the nanoplates

The crystal structure of the as-prepared nanoplates is analyzed by XRD, as shown in Fig. 1. All the strong diffraction peaks for the two XRD patterns can be indexed to a typical hexagonal α-$NaFeO_2$-type structure with a space group *R-3m* [18], except for the weak peaks in the 2θ range of 20–25°. These weak peaks are caused by lithium-cation ordering in the transition-metal layers. It is the features of the integrated monoclinic Li_2MnO_3 phase (*C*2/*m*) [19]. In addtion, both the pair reflections (006)/(012) and (018)/(110) of the two samples split very well. This indicates the two samples have good hexagonal ordering and well-formed layered structure [20]. Generally, the ratio of I_{003}/I_{104} can reflect the degree of the cation mixing in the Li-layers of LLOs, and undesirable cation mixing would occur in the lattice when the ratio of I_{003}/I_{104} is less than 1.2 [21]. In XRD patterns of the samples S101 and S001, the ratios of I_{003}/I_{104} respectively are 2.29 and 2.41, much over 1.2. It proves cation mixing in the two samples is very low.

Chemical compositions of the two samples are analyzed by ICP. As listed in Table 1, the two samples show very close compositions. Herein, chemical composition has a little effect on the electrochemical performance of the two samples. In addition, morphology of the two samples is detected by scanning electron microscopy (SEM). As displayed in Fig. 1a,b and Fig. S1, both the two samples are composed of many nanoplates. Clearly, the particle size of the two nanoplates is very close. Their thickness and inscribed circle diameter respectively lie in 50–100 and 200–300 nm.

The morphology and structure are further characterized by transmission electron microscopy (TEM) and selected-area electron

Download English Version:

https://daneshyari.com/en/article/5148690

Download Persian Version:

https://daneshyari.com/article/5148690

Daneshyari.com